Supporting Information

Engineering Interfacial Silicon Dioxide for Improved MIS Silicon Photoanode Water Splitting Performance

Peter F. Satterthwaite[a], Andrew G. Scheuermann[a], Paul K. Hurley[b], Christopher E. D. Chidsey[c], Paul C. McIntyre[,a]*

[a] Department of Materials Science and Engineering, Stanford University, Stanford, CA, United States

[b] Tyndall National Institute, University College Cork, Cork, Ireland

[c] Department of Chemistry, Stanford University, Stanford, CA, United States

*Corresponding Author, E-mail: pcm1@stanford.edu

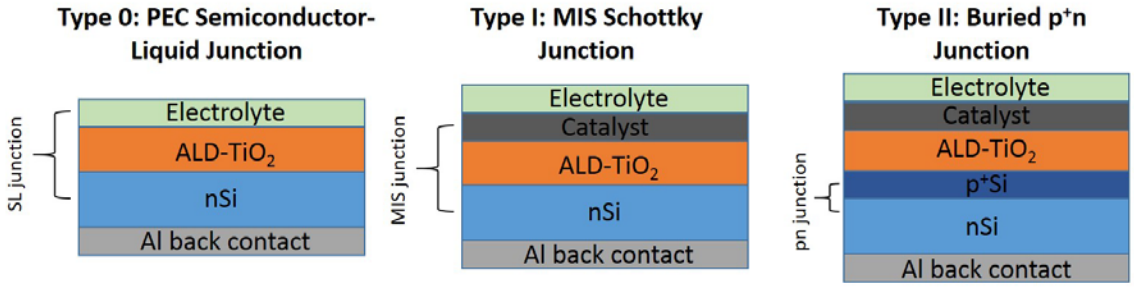

Figure S1 | Photovoltaic-Based PEC Cell Types The three types of junctions routinely utilized for photoelectrochemistry shown with the example of ALD-TiO_2 protection of silicon photoanodes. Type 0 photoelectrosynthetic cells[1] generate voltage from a semiconductor-liquid junction typically using a stable metal-oxide layer on the semiconductor substrate. Type 1 photovoltaic-biased photoelectrosynthetic cells[1] generate voltage from a metal—insulator-semiconductor (MIS) Schottky junction with an interposed protection layer. Type 2 photovoltaic-biased photoelectrosynthetic cells[1] generate voltage with a buried p^+n junction with the metal oxide protection layer and catalyst in series. Type 2 photoanode cells are often realized by doping the top portion of an n-type substrate to create a thin p^+ region.

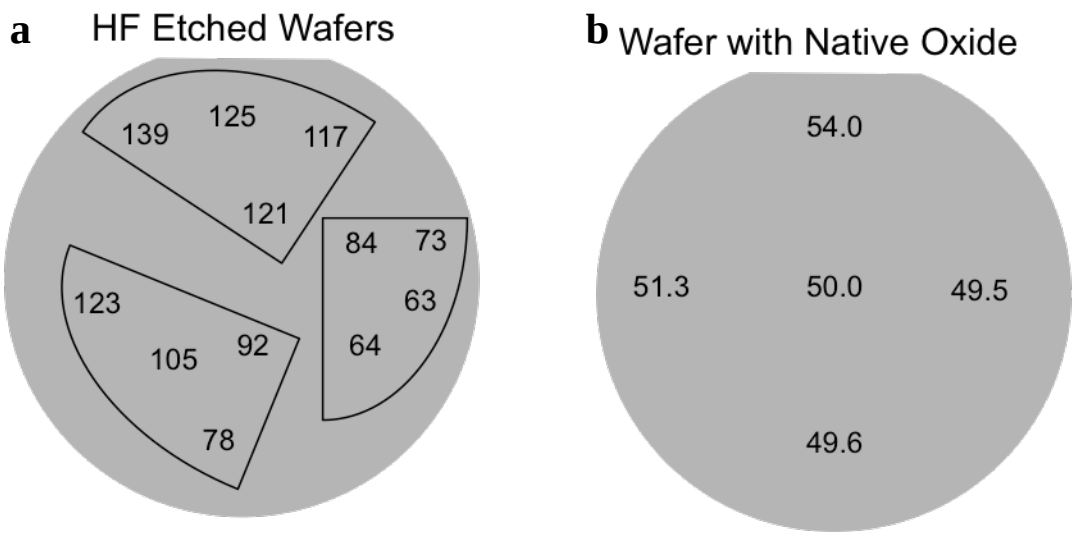

Figure S2 | Thickness of TiO_2 deposition by ALD on an HF-last surface and vendor chemical oxide. Deposition on HF last surface **(a)** shows much higher thickness variation than qualification run performed on the same silicon substrate with the chemical oxide in place **(b)** immediately after using the same chamber conditions on the vendor chemical oxide for a 100 cycle run.

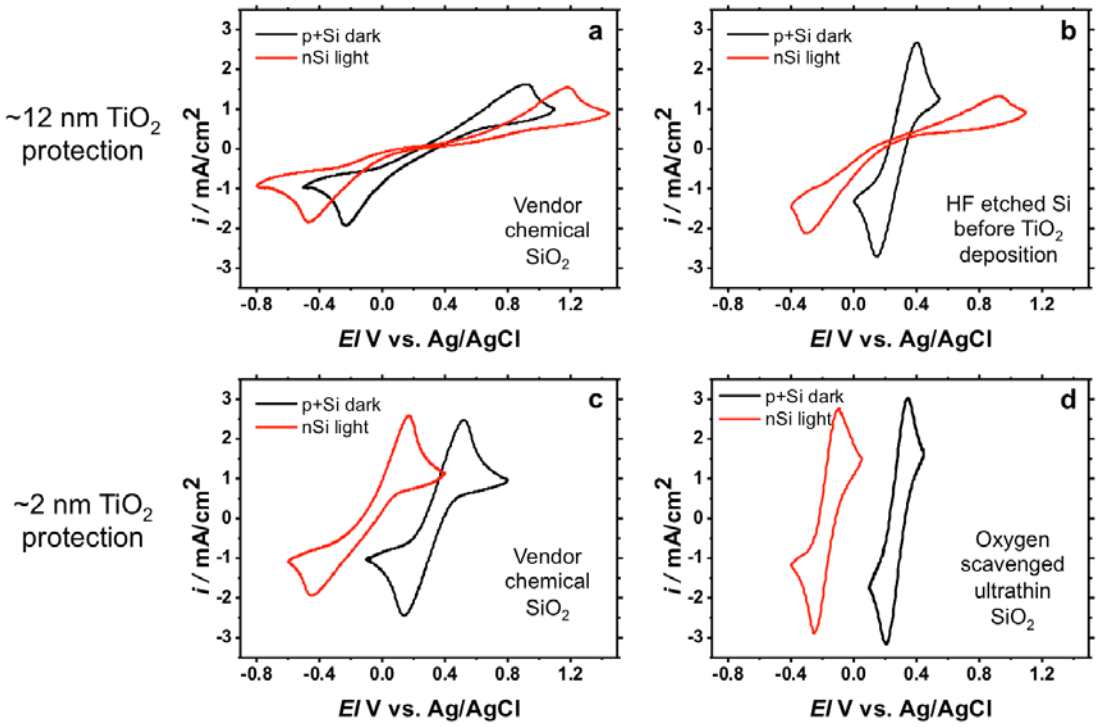

Figure S3 | Photovoltage comparisons for various 2 nm Ir/TiO_2/SiO_2/silicon anodes, with a range of thin SiO_2 configurations which can be measured as the shift of the p^+Si anodes measured in the dark (black trace) to the nSi photoanodes measured in 1 sun of AM 1.5G illumination (red trace). **(a)** ~12 nm TiO_2/vendor chemical-oxide/Si showing the zero to negative photovoltage observed in these systems with moderately leaky TiO_2 **(b)** ~12 nm TiO_2/HF-last Si showing much increased conductivity for the p^+Si anode but a flattened nSi curve suggesting strong recombination limiting the anodic current. This is likely due to a poor quality interface with high trap density leading to increased trap-mediated recombination. **(c)** ~2 nm TiO_2/vc-oxide/Si showing an ~500 mV photovoltage with moderately leaky TiO_2 giving some residual resistance stretching out the CV. **(d)** ~2 nm TiO_2/scavenged vc-oxide/Si showing a strong photovoltage shift of 500-550 mV and near-ideal conductivity of both the dark anode and the illuminated Schottky junction nSi photoanode**.**

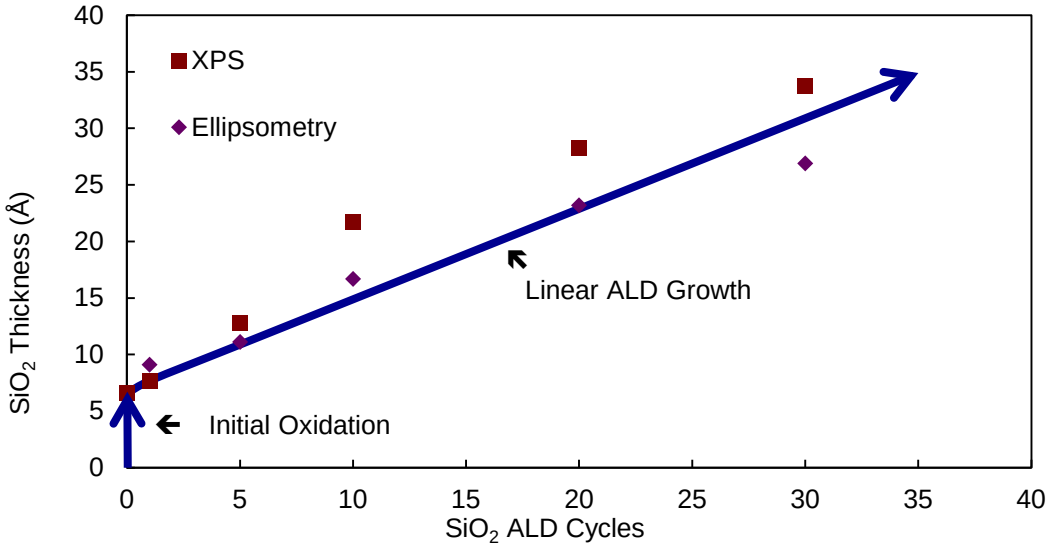

Figure S4 | SiO_2 ALD thickness measured from XPS and ellipsometry. The purple diamonds represent thicknesses characterized ellipsometrically. The red squares represent thickness characterization performed via XPS analysis and equation (1). The blue vertical line at zero ALD cycles of SiO_2, represents initial oxidation of the HF-last surface, and subsequent linear ALD growth is ~0.8 Å/cycle, as is typical for this process. The 0 cycle sample displays a non-zero SiO_2 thickness representing oxidation resulting during the TiO_2 ALD process on an HF-last surface as discussed in the manuscript.

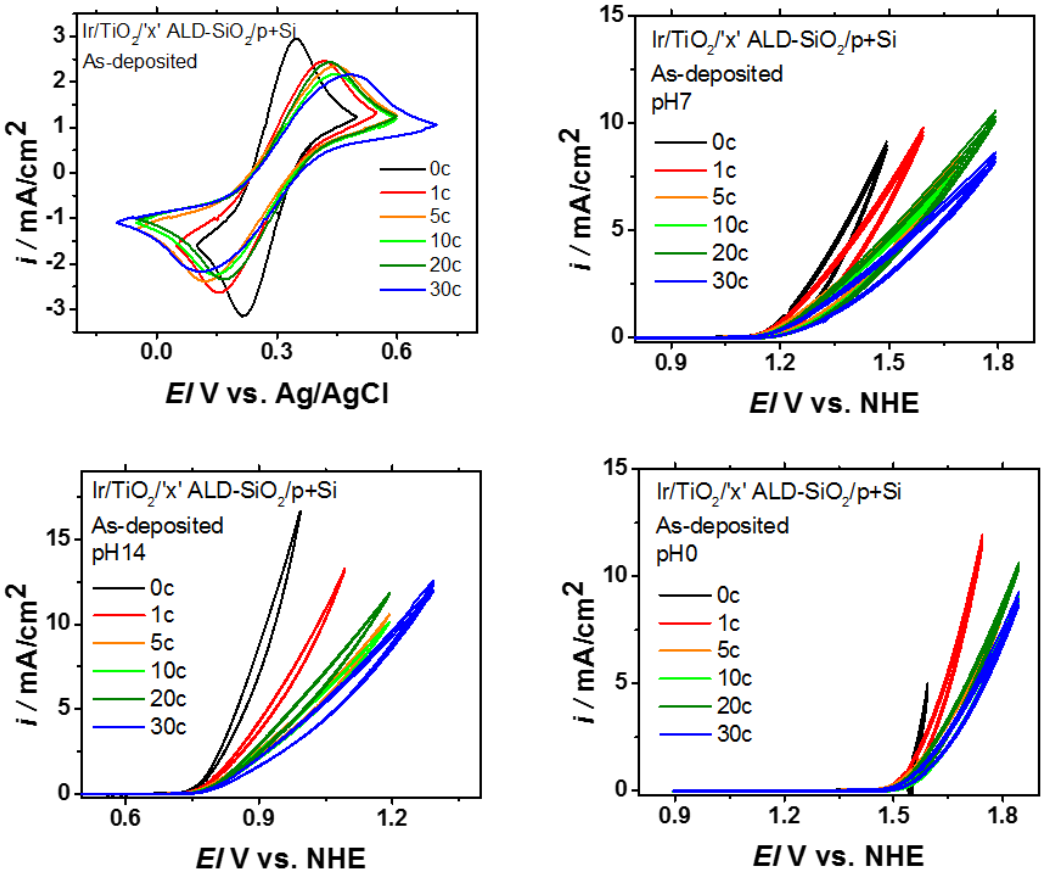

Figure S5 | Ir / ~ 2 nm TiO_2 / 'x' cycles of ALD-SiO_2 / p^+Si electrochemistry results. The results in ferri/ferrocyanide, pH 14 1M NaOH, pH 7 phosphate buffer, and pH 0 1M H_2SO_4 are shown here demonstrating the slowly scaling increased turn-on overpotentials at 1mA/cm^2 shown in figure 5.

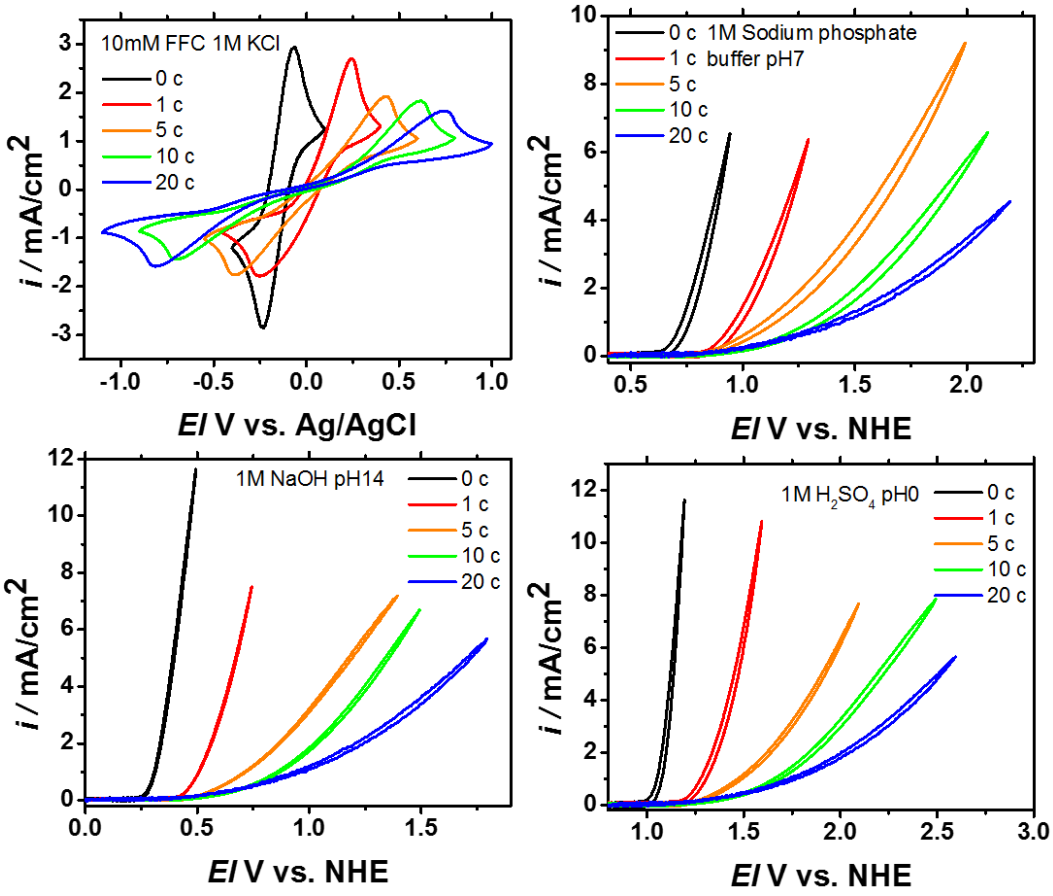

Figure S6 | Ir / ~2 nm TiO_2 / 'x' cycles ALD-SiO_2 / nSi electrochemistry results. The results in ferri/ferrocyanide, pH 14 1M NaOH, pH 7 phosphate buffer, and pH 0 1M H_2SO_4 are shown here demonstrating the much more rapidly scaling overpotential loss as shown in Figure 5 (main paper) for the Schottky nSi photoanodes. Figure 4 (main paper) resistance modelling is performed from the ferri/ferrocyanide nSi profiles shown in the upper left quadrant.

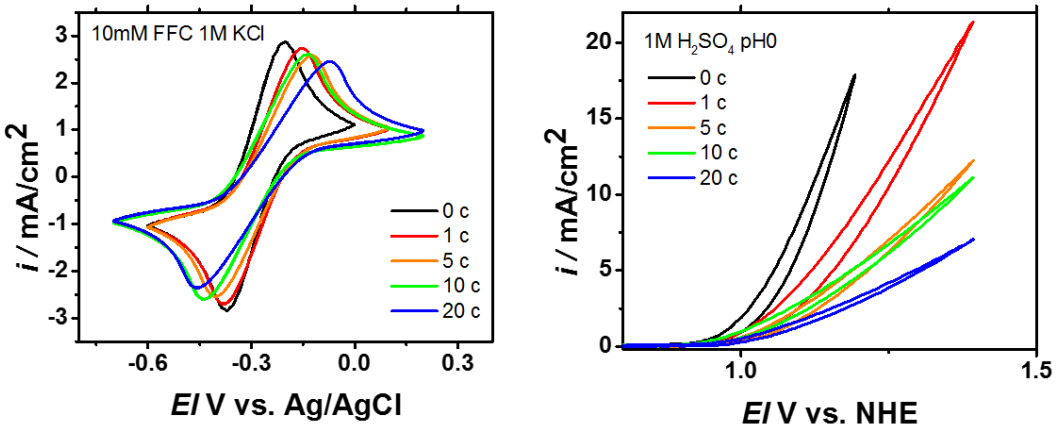

Figure S7 | Ir / ~2 nm TiO_2 / 'x' cycles ALD-SiO_2 / p^+n Si electrochemistry results. The results in ferri/ferrocyanide and pH 0 1M H_2SO_4 are shown here demonstrating the slowly scaling increased turn-on overpotentials for buried junction p^+nSi photoanodes similar to the p^+Si reference anodes where only an Ohmic resistance remains from the extra interlayer insulators as opposed to the photovoltage loss seen in Figure S6 by the nSi Schottky junction photoanodes.

Supporting References

(1) Nielander, A. C.; Shaner, M. R.; Papadantonakis, K. M.; Francis, S. A.; Lewis, N. S. A Taxonomy for Solar Fuels Generators. *Energy Environ. Sci.* **2015**, 8 (1), 16-25.